Electronic Supplementary Material (ESI) for Physical Chemistry Chemical Physics.

Supporting Information for

Cation-responsive cavity expansion of valinomycin revealed by cryogenic ion trap infrared spectroscopy

Keisuke Hirata[†‡], Eiko Sato,[†ǁ] James M. Lisy,*[⊤⊥] Shun-ichi Ishiuchi*[†‡] and Masaaki Fujii*[†‡⊤]

[†]Laboratory for Chemistry and Life Science, Institute of Innovative Research, Tokyo Institute of Technology. 4259 Nagatsuta-cho, Midori-ku, Yokohama, 226-8503, Japan.

[‡]Department of Chemistry, School of Science, Tokyo Institute of Technology, 2-12-1 Ookayama, Meguro-ku, Tokyo 152-8550, Japan.

[ǁ]School of Life Science and Technology, Tokyo Institute of Technology. 4259 Nagatsuta-cho, Midori-ku, Yokohama, Kanagawa, 226-8503, Japan.

[⊤]International Research Frontiers Initiative (IRFI), Institute of Innovative Research, Tokyo Institute of Technology, 4259, Nagatsuta-cho, Midori-ku, Yokohama, 226-8503, Japan.

[⊥]Department of Chemistry, University of Illinois at Urbana-Champaign, Urbana, IL 61801, USA

ORCID ID

KH:0000-0003-4472-7992, JL:0000-0002-9894-9163, SI: 0000-0002-4079-818X, MF: 0000-0003-4858-4618

[*] Corresponding authors

JML: j-lisy@illinois.edu, SI: ishiuchi.s.aa@m.titech.ac.jp, MF: mfujii@res.titech.ac.jp

Experimental and computational methods

IR photodissociation (IRPD) spectra of valinomycin-metal complexes (M^+VM) were measured in a cryogenic ion trap setup (Figure S1).[1] Methanol solutions of VM (Wako, 10^{-5} M) and the desired alkali metal chloride (Wako, 2×10^{-5} M) were electrosprayed via a glass capillary heated to 60°C (where the solvent is driven off), and allowing the ion-neutral complexes to enter the vacuum apparatus through a skimmer. The specific ions of interest were transported by a hexapole ion guide, mass-selected by a quadrupole mass spectrometer (Extrel), deflected by a quadrupole bender, and then guided into a cryogenic quadrupole ion trap (QIT) in which electrodes are made of copper with gold coating. The QIT was cooled to 4 K by a closed cycle He refrigerator (Sumitomo, RDK-408D2). A mixture of hydrogen (20%) and helium buffer gas was introduced to the QIT via a pulsed nozzle (Parker Hannifin: General Valve Series 9) and cooled down by collisions with the QIT's electrodes. The complex ions were trapped and cooled to ~10 K (vibrational temperature) by collisions with buffer gas. Hydrogen molecules were condensed onto the cold ions, forming a variety of weakly-bound hydrogen-attached cluster ions. The cluster ions were then irradiated with a tunable IR laser (LaserVision: OPO/OPA laser). Absorption of a photon triggers the dissociation of the weakly-bound hydrogen molecules from the cluster ions, yielding the parent M^+VM complex ion as a photofragment. The IRPD spectrum of the trapped ions was measured by monitoring the photofragment signals by a time-of-flight mass spectrometer (TOF-MS). The photofragment signals from a dynode converter detector of TOF-MS were amplified ten times by a preamplifier and recorded on a fast digitizer. The IRPD spectra were measured by scanning the wavenumber of the IR laser.

Calculated vibrational frequencies presented in this study were obtained from density functional theory (DFT) calculations using the dispersion-corrected B3LYP-D3BJ functional and the lanl2dz (Rb, Cs)/6-31G(d,p) (C, N, O, H) basis sets, which are used in the studies on K^+VM and $K^+VM(H_2O)_1$.[2] This set of functional and basis sets well reproduced the IRPD spectra of K^+VM and $K^+VM(H_2O)_1$.[2] The DFT calculations were performed using the Gaussian 16 package.[3] Initial structures were prepared based on the geometry data of the crystal structures of K^+VM (bracelet-type conformation[4]) and bare VM (twisted bracelet- and propeller-type conformations[5, 6]) and are shown in Figure S2. All the optimized structures were confirmed to be local minima with no imaginary vibrational frequencies. The calculated frequencies have been corrected for anharmonicity with a scaling factor of 0.961, identical to the previous report on the K^+VM complex.[2] The calculated IR spectra were convoluted with a Lorentz lineshape function with a half width of 3 cm^{-1} (typical energy resolution of the IR laser). The binding energy (E_{BE}) between metal and VM was calculated at the B3LYP-D3BJ/def2-SVP level using Eq. 1.

$$E_{!"} = (G_{\#} + G_{\$\#}) - (G_{\#\$\#} + BSSE) \quad (1)$$

The *BSSE* value corresponds to the correction term of basis set superposition error (BSSE). This value

was calculated by the counterpoise method. G_M, G_{VM}, and G_{MVM} represent Gibbs free energy for a metal ion, VM, and the complex of the metal and VM at 298 K, respectively.

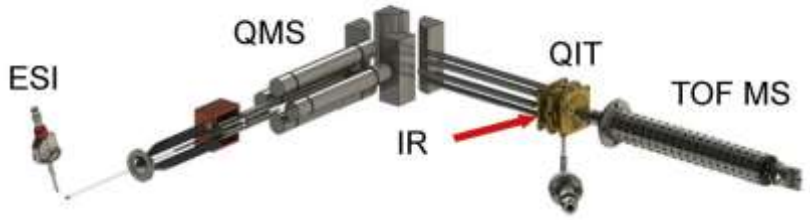

Figure S1 Experimental setup.[1] ESI: Electrospray Ionization source, Q-MS: Quadrupole mass spectrometer, QIT: Quadrupole ion trap, TOF MS: Time-of-flight mass spectrometer.

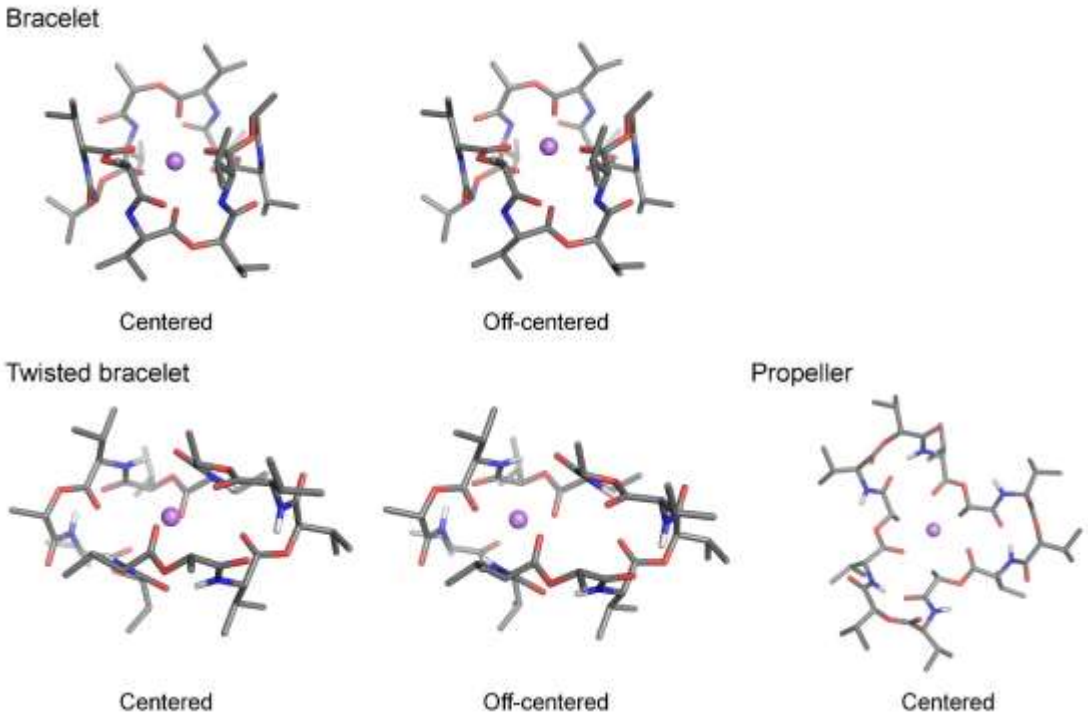

Figure S2 Initial structures of M^+VM used in this study. The frameworks of valinomycin (VM) are taken from the crystal structures of K^+VM (bracelet-type conformation) and bare VM (twisted bracelet- and propeller-type conformations). A metal ion is located at the center and off-centered positions.

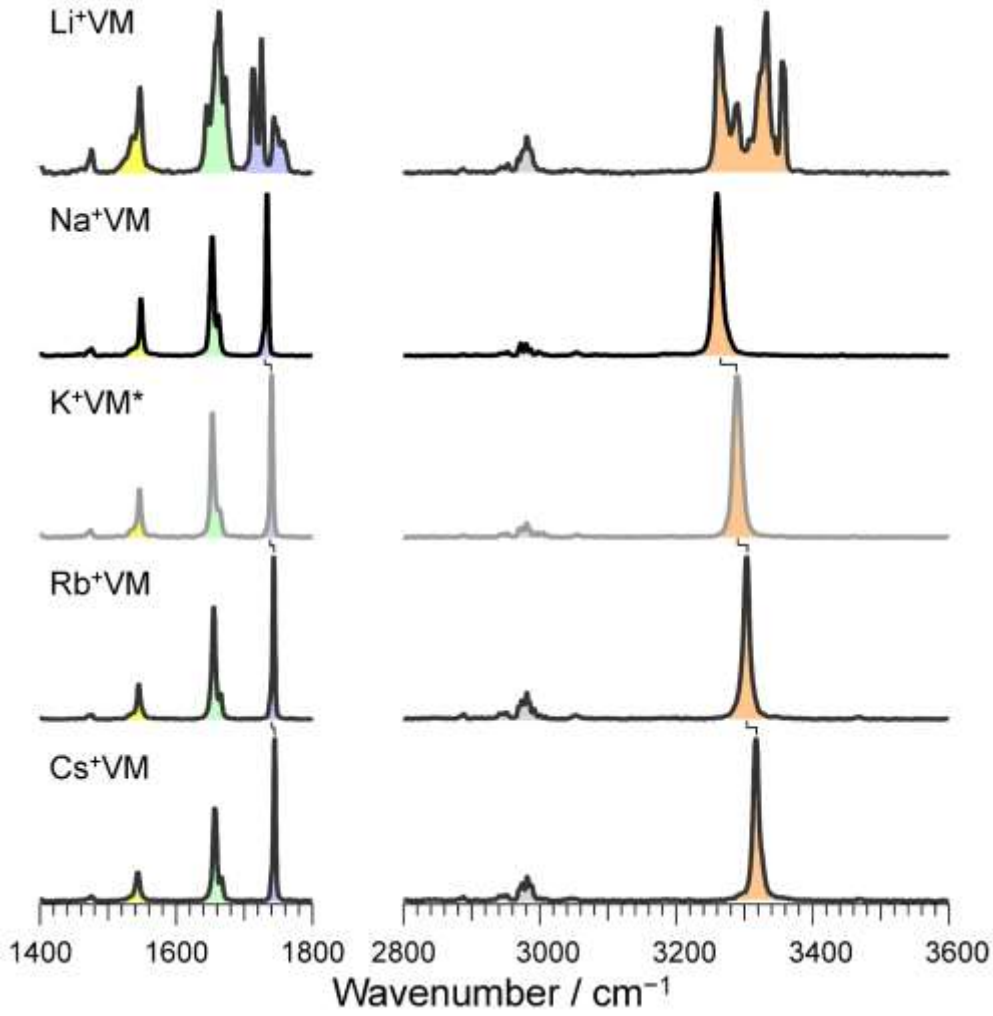

Figure S3 IRPD spectra of VM-alkali metal complexes. The areas colored in orange, gray, purple, green, and yellow correspond to NH stretch, CH stretch, ester CO stretch, amide CO stretch, and amide NH bend, respectively. The IRPD spectrum of K^+VM marked in asterisk is reported in ref 2.

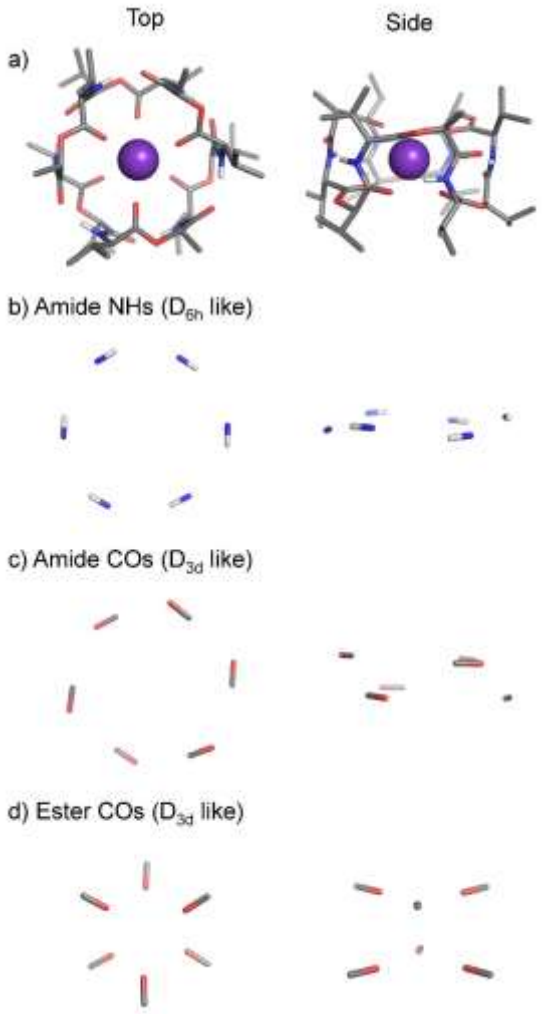

Figure S4 a) Top and side views of the K^+VM complex. Top and side views of the configurations of b) amide NHs, c) amide COs, and d) ester COs. The amide NHs are aligned on a plane with almost D_{6h} symmetry. Amide COs no longer holds σ_h plane and its configuration is degraded to D_{3h}-ilke symmetry. The configuration in ester COs are also classified as D_{3d}-like symmetry.

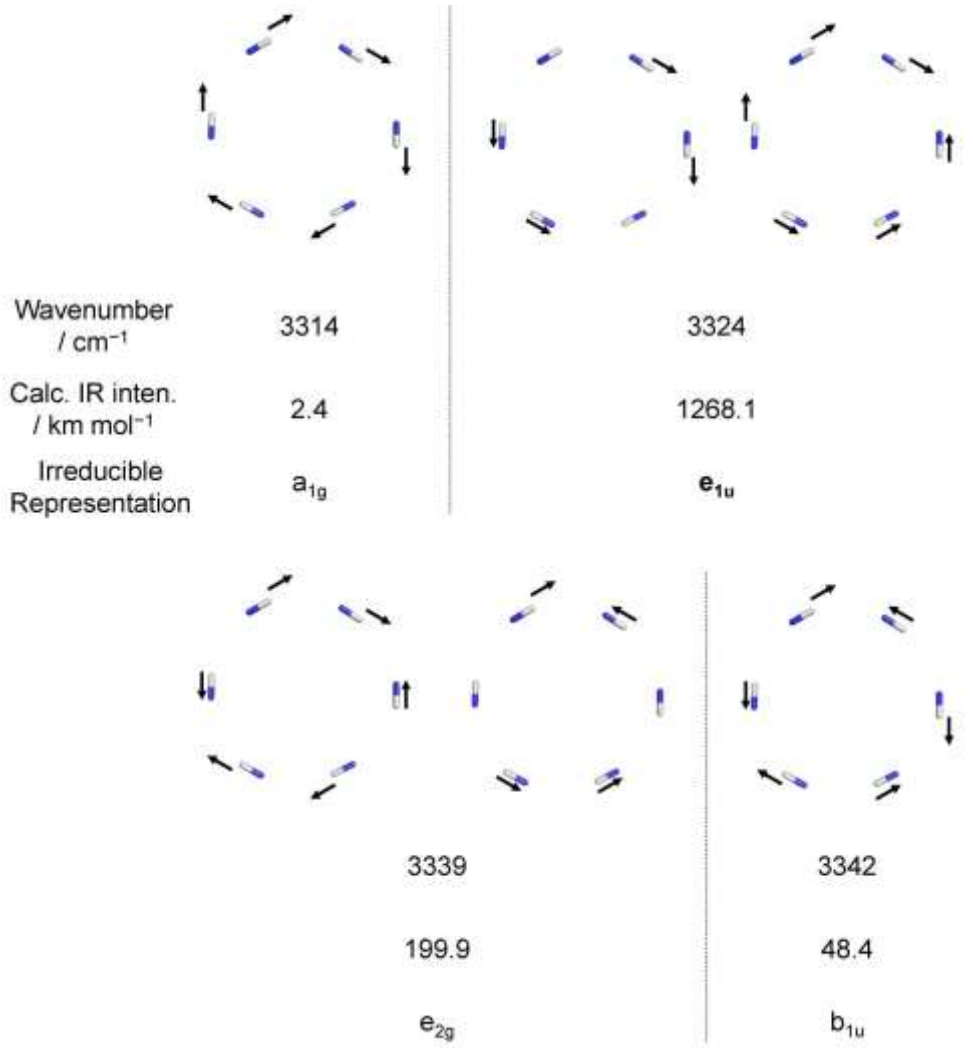

Figure S5 Calculated vibrations of amide NH stretches for K^+VM with the wavenumbers, IR intensities, and corresponding irreducible representations. Wavenumbers are scaled by 0.961. Bold and non-bold letters in irreducible representations indicate allowed and forbidden IR transitions, respectively.

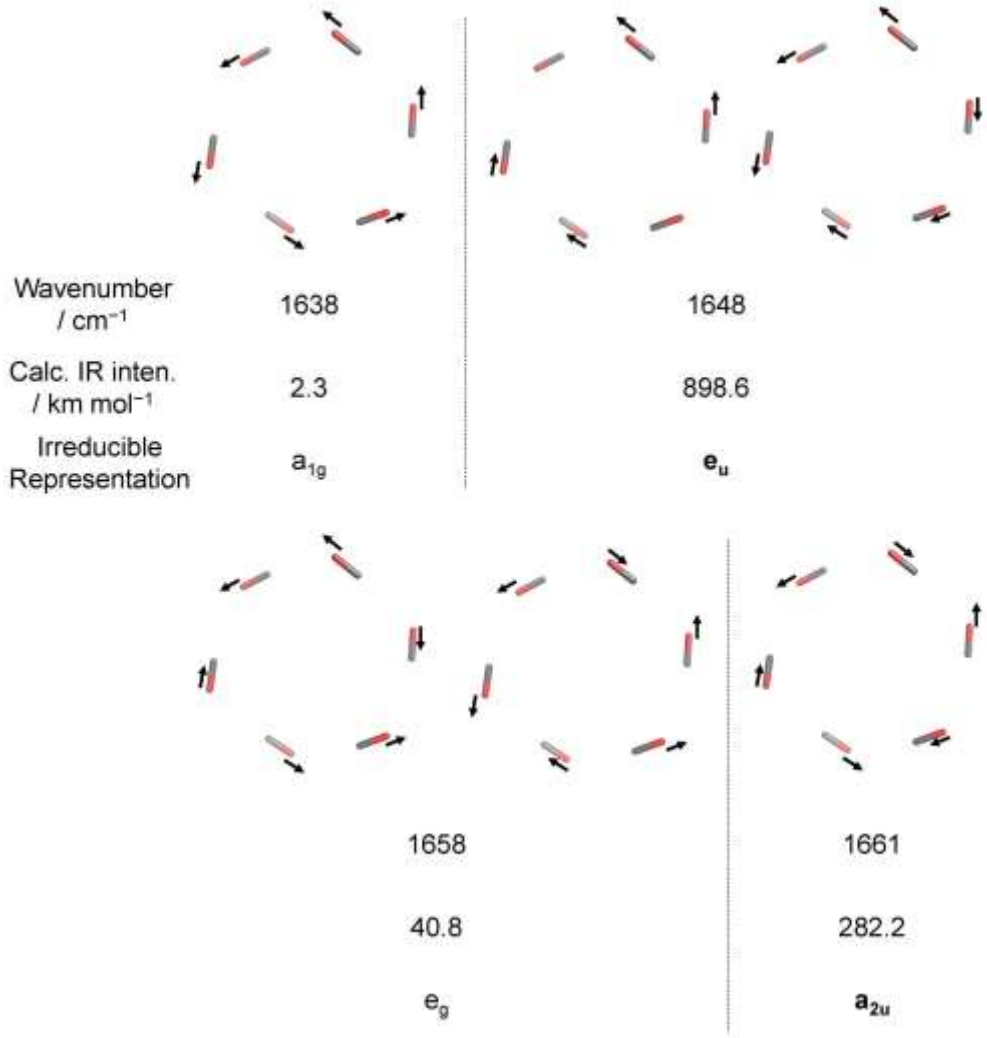

Figure S6 Calculated vibrations of amide CO stretches for K^+VM with the wavenumbers, IR intensities, and corresponding irreducible representations. Wavenumbers are scaled by 0.961. Bold and non-bold letters in irreducible representations indicate allowed and forbidden IR transitions, respectively.

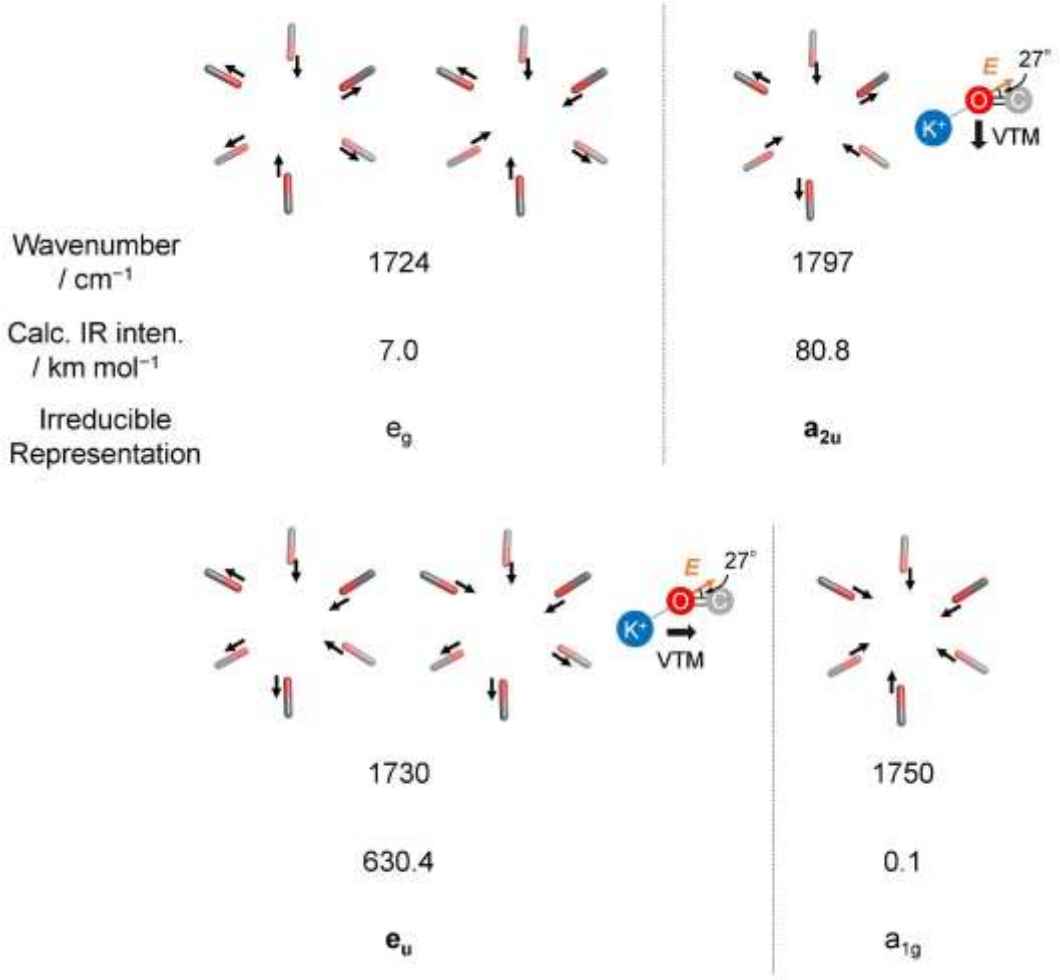

Figure S7 Calculated vibrations of ester CO stretches for K^+VM with the wavenumbers, IR intensities, and corresponding irreducible representations. Wavenumbers are scaled by 0.961. Bold and non-bold letters in irreducible representations indicate allowed and forbidden IR transitions, respectively. The schematics indicate the vibrational transition dipole moment (VTM) and electric field (*E*) generated by K^+. The averaged angle (°) between O=C and *E* are shown in the schematics.

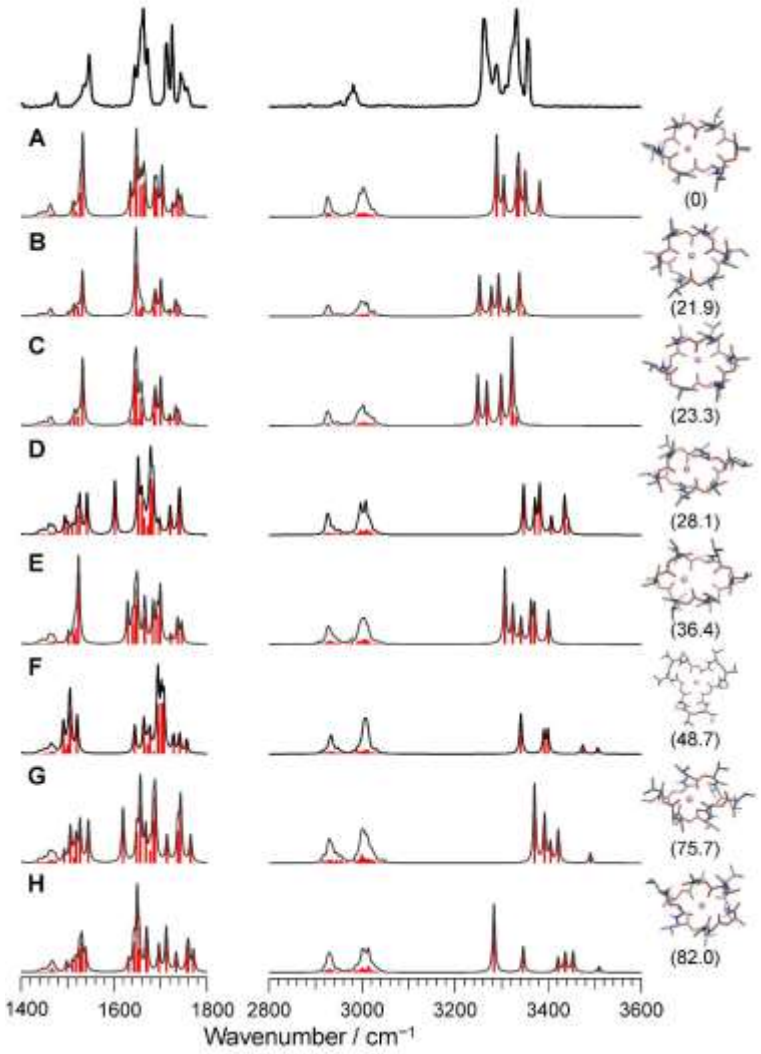

Figure S8 Calculated IR spectra of conformers A–H for Li^+VM with the experimental IRPD spectrum. The most red-shifted NH stretches band of Conf. E and G are more intense than the other NH stretches, which does not match with the experimental IRPD spectrum. The bands at >3500 cm^{-1} for Conf. F and H do not coincide with the experimental feature. There are substantial differences for Conf. B to H in the 1400-1800 cm^{-1} region involving the NH bend, amide CO and ester CO stretches, in comparison to the experimental spectrum, as well.

Table S1 Logarithm of the equilibrium constants (log *K*) for the complexation of valinomycin/18-crown-6 and an alkali metal.[7]

	Li^+	Na^+	K^+	Rb^+	Cs^+
Valinomycin	<0.7	0.67	4.90	5.26	4.41
18-crown-6	~0	4.36	6.06	5.32	4.79

Table S2 Vibrational frequencies of the bands observed in the IRPD spectra of M^+VM.

	CH bend	NH bend	Amide CO	Ester CO	CH stretch	NH stretch
Li^+VM	1476	1536	1645	1713	2954	3263
		1547	1663	1725	1981	3290
			1672	1744		3233
				1757		3256
Na^+VM	1475	1548	1653	1733	2953	3260
			1662		2973	
					2980	
					2987	
Rb^+VM	1475	1545	1655	1743	2943	3304
			1666		2981	
Cs^+VM	1476	1544	1657	1744	2942	3317
			1667		2982	

Table S3 Distances (*d*) between metal and six oxygens of ester carbonyl for the optimized structures of M^+VM. Red value corresponds to the elongated distance characteristic to Conformer B in Na^+VM.

		d / Å
Li^+VM	Conf. A	1.95 / 1.96 / 1.98 / 2.02 / 4.40 / 4.44
	B	1.98 / 2.05 / 2.06 / 2.16 / 3.80 / 3.86
	C	1.99 / 2.05 / 2.06 / 2.12 / 3.75 / 4.03
	D	1.94 / 1.94 / 2.06 / 2.08 / 4.55 / 5.50
Na^+VM	Conf. A	2.50 / 2.50 / 2.51 / 2.51 / 2.54 / 2.59
	B	2.46 / 2.47 / 2.47 / 2.49 / 2.49 / 2.83
	C	2.28 / 2.36 / 2.39 / 2.45 / 2.52 / 3.46
	D	2.41 / 2.43 / 2.43 / 2.43 / 2.83 / 3.29
K^+VM		2.72 / 2.72 / 2.72 / 2.72 / 2.72 / 2.72
Rb^+VM		2.85 / 2.85 / 2.85 / 2.86 / 2.86 / 2.86
Cs^+VM		3.02 / 3.02 / 3.02 / 3.02 /3.03 / 3.03

Table S4 Distances (*d*) and binding energy (E_{BE}) for the C_3-symmetric bracelet structures of M^+VM.

	d (M^+…OC) / Å [a]	*d* (NH…OC) / Å [b]	E_{BE} / kJ mol^{-1}
Na^+VM	2.53	1.82	98.1
K^+VM	2.72	1.87	83.0
Rb^+VM	2.86	1.91	74.8
Cs^+VM	3.02	1.96	64.1

[a] Averaged distance between metal and ester (C)O. [b] Averaged distance between amide NH and amide (C)O.

References

1. S. Ishiuchi, H. Wako, D. Kato and M. Fujii, *J. Mol. Spectrosc.*, 2017, **332**, 45-51.
2. E. Sato, K. Hirata, J. M. Lisy, S. Ishiuchi and M. Fujii, *J. Phys. Chem. Lett.*, 2021, **12**, 1754-1758.
3. M. J. Frisch, G. W. Trucks, H. B. Schlegel, G. E. Scuseria, M. A. Robb, J. R. Cheeseman, G. Scalmani, V. Barone, G. A. Petersson, H. Nakatsuji, et al., Gaussian 16, Gaussian, Inc. Wallingford, CT2016.
4. K. Neupert-Laves and M. Dobler, *Helv. Chim. Acta*, 1975, **58**, 432-442.
5. I. L. Karle, *J. Am. Chem. Soc.*, 1975, **97**, 4379-4386.
6. I. L. Karle and J. L. Flippen-Anderson, *J. Am. Chem. Soc.*, 1988, **110**, 3253-3257.

7. R. M. Izatt, J. S. Bradshaw, S. A. Nielsen, J. D. Lamb, J. J. Christensen and D. Sen, *Chem. Rev.*, 1985, **85**, 271-339.